9^{th} South African Conference on Computational and Applied Mechanics
Somerset West
14 – 16 January 2014

An Investigation into the Applicability of the Lattice Boltzmann Method to Modelling of the Flow in a Hydrocyclone

M. Bhamjee[1], S.H. Connell[2], A.L. Nel[3]

[1,3] Department of Mechanical Engineering Science, Faculty of Engineering and the Built Environment, University of Johannesburg; [1]muaazb@gmail.com; [3]andren@uj.ac.za;

[2] Department of Physics, Faculty of Science, University of Johannesburg; shconnell@uj.ac.za

Abstract: The lattice Boltzmann method has gained popularity as a method for simulating fluid flow, particularly multiphase flow. Thus, it has potential in simulating fluid flow in hydrocyclones. While research on the method and its' application to multiphase flow is mature, there is sparse research on its' application to hydrocyclones. An overview of the literature on the use of the lattice Boltzmann method for simulating fluid flow in hydrocyclones is presented. A lattice Boltzmann model of single phase flow in a hydrocyclone is presented, which is compared to predictions from a Navier-Stokes based model. The lattice Boltzmann model predicts lower velocities than the Navier-Stokes model in certain areas of the hydrocyclone and higher velocities in other areas. In some areas both models are in close agreement. The lattice Boltzmann model predicts the low pressure region at the underflow and overflow. However, it does not display the low pressure region in the core of the hydrocyclone. It is proposed that these differences are related to the use of the single relaxation time implementation of the lattice Boltzmann method. The possible solution is to use the multiple relaxation time model which is more suitable to high-Reynolds number flows.

Keywords: Hydrocyclone, LBM, CFD, Multiphase, Air-Core, LES

Introduction

The Lattice Boltzmann Method (LBM) has gained popularity as an alternative method, to the Navier-Stokes (NS) based Finite Volume Method (FVM), for simulating fluid flow [1–4]. Furthermore, with its high level of parallelism [4] it has significant advantages over the NS based FVM in terms of computational cost. Thus, it has major potential for applications in industry. Its' popularity, however, remains within the academic sphere and has made slow progress in becoming a commonly used technique in industry in relation to the NS based FVM [1]. It is particularly adept at solving multiphase and discrete phase problems which is of particular interest in simulating process equipment such as cyclone separators [1–4]. However, the literature on the application of the LBM to hydrocyclones is sparse [4, 5]

Gronald and Derksen [4] have shown that for single phase flow the LBM is comparable to the NS based FVM with regards to hydrocyclone modelling. However, Gronald and Derksen [4] provide insufficient information on how they applied the LBM. Thus, it is not possible to reconstruct a working model of a hydrocyclone from the work of Gronald and Derksen [4].

Pirker *et al.* [5] used a hybrid of the NS based FVM and LBM to model a gas-cyclone short-cut flow. The hybrid model used in [5] comprised of the NS based FVM which was used to model the cyclone except the annulus region (intake). The annulus region at the top of the cyclone was modelled using the LBM [5]. The LBM used in Pirker [5] including the LES turbulence model. The NS based FVM model was used in a separate case, throughout the domain, to compare with the LBM. The LBM showed superior predictions to the NS based FVM relative to experimental data [5]. Thus, it may be of benefit to model an entire cyclone/ hydrocyclone using the LBM.

It is clear that the literature on the application of the LBM to modelling fluid flow in hydrocyclones is not sufficient to reconstruct an LBM model of a hydrocyclone. Thus, the aim of this study is to present an LBM model of single phase flow in a hydrocyclone. The model predictions will be compared to the predictions from an NS based FVM model of the hydrocyclone. The LBM model and its' implementation will be described in detail.

Nomenclature

B_i	Body force components $\forall i = x, y, z$
C_s	Smagorinsky constant
c	Speed of sound, m/s
$\mathbf{c}_i$	Lattice vector
c_s	lattice speed of sound
D_H	Hydraulic diameter, m
f	Single-particle distribution function
f^{eq}	Equilibrium distribution function
$\mathbf{g}$	Gravitational vector, m/s^2
g	Gravitational constant, m/s^2
I_{turb}	Turbulence intensity, $\%$
$\dot{m}$	Mass-flow rate, kg/s
P_a	Atmospheric pressure, kPa
$\bar{p}$	Mean pressure, Pa
p	Instantaneous pressure, Pa
p'	Fluctuating pressure due to turbulence, Pa
p_{gauge}	Gauge pressure, kPa
r	Radius, m
S	Strain-rate tensor
$\|S\|$	Tensor norm of strain-rate tensor
t	Time, s
Δt	Time step size, s
δt	Discrete time unit, s
u	Velocity, m/s
$\bar{\mathbf{u}}$	Mean velocity vector, m/s
$\overline{u_i}$	Mean velocity components $\forall i = x, y, z$, m/s
$\mathbf{u}$	Velocity vector, m/s
u_i'	Fluctuating velocity components $\forall i = x, y, z$, m/s
u_i	Instantaneous velocity components $\forall i = x, y, z$, m/s
v_θ	Tangential velocity, m/s
x, y, z	Cartesian co-ordinates, m
x_i	Cartesian directions $\forall i = x, y, z$, m
Δx	Lattice spacing, m
w_i	Lattice weights
$\mathbf{0}$	Zero vector

Greek Symbols

μ	Viscosity, $kg/(m.s)$
ν	Kinematic viscosity, m^2/s
ξ	Microscopic Velocity, m/s
$\rho\overline{u_i'u_j'}$	Reynolds stresses (Tensor Notation), Pa
ρ	Density, kg/m^3
τ_0	Relaxation time, s
τ_t	Turbulent (LES) relaxation time, s
τ_*	Effective relaxation time, s

Table 1: Fluid Properties.

Fluid	ρ $(\mathbf{kg/m^3})$	μ $(\mathbf{kg/(m.s)})$
Water	1000	$1.003(10^{-3})$

NS Model

Governing Equations

The NS based CFD model was implemented using ANSYS Fluent [6]. The flow field for the water is described by the continuity equation and the Reynolds Averaged Navier - Stokes (RANS) equations for incompressible flow with gravity as the only body force ($B_x = 0$, $B_y = 0$, $B_z = -\rho g$). The continuity and RANS equations are given by Equations 1 and 2, respectively [7–12].

$$\nabla.(\bar{\mathbf{u}}) = 0 \tag{1}$$

$$\rho\frac{\partial \bar{u}_i}{\partial t} + \rho\nabla.(\bar{u}_i\bar{\mathbf{u}}) = -\frac{\partial \bar{p}}{\partial x_i} + \nabla.(\mu \text{ grad } \bar{u}_i) - B_i - \rho\frac{\partial}{\partial x_i}(\overline{u_i'u_j'}) \tag{2}$$

The turbulence model used, to provide closure to the RANS Equations, is the Reynolds Stress Model (RSM). The transport equations for the RSM, for incompressible flow are extensive. Thus, the interested reader may consult [10,13] for a detailed presentation of the RSM transport equations. The Stress-Omega pressure strain term was employed due to it's proven accuracy for highly swirling flows [10]. The density and viscosity, specified in the model, for the water is given in Table 1.

Model Geometry, Mesh and Boundary Conditions

An isometric view of the hydrocyclone geometry (CFD domain) is shown in Figure 1. The salient dimensions of the hydrocyclone are given in Table 2. The salient boundary conditions for the CFD model are detailed in Table 3. Atmospheric Pressure (P_a) is taken as $P_a = 82.5\ kPa$ which is realistic for Johannesburg. The no-slip condition was specified at the wall boundaries.

A radial equilibrium pressure distribution is applied at the underflow and overflow. Thus, the gauge pressure ($p_{gauge} = 0\ kPa$) is applied at the center of both the outlets. The static pressure on the rest of the boundary is calculated using [14]:

$$\frac{\partial p}{\partial r} = \frac{\rho v_\theta^2}{r} \tag{3}$$

The computational grid (mesh) was constructed with a cell size of $5\ mm$ in all regions using the sweep and multizone meshing schemes. However, the inlet has a sloping and reducing section which was meshed using the tetrahedral cell type with a cell size of $5\ mm$. The mesh consisted of approximately 123908 cells. A second mesh with a grid spacing of $2.5\ mm$ was also used. This resulted in a mesh of 928516 cells.

Solver Setup

The ANSYS Fluent three-dimensional, unsteady, double precision solver was used for the NS based model. The pressure based coupled solver was used. The discretisation scheme used for the momentum, energy, turbulent kinetic energy and Reynold Stress equations was the QUICK scheme. PRESTO! was used for the pressure discretisation scheme. Gradient reconstruction was done using the least squares cell based method.

The under-relaxation factors were kept at their default settings as per [14]. The fixed time step size was $\Delta t = 10^{-4}\ s$. This time step size resulted in the models converging in 5 - 15 iterations per time step. The acceptable residual limits for continuity, x, y and z momentum, turbulent kinetic energy and Reynold Stresses were $< 10^{-3}$ [10,14]. Monitors for mass-flow rate on the overflow and underflow were used to determine when steady state conditions were reached.

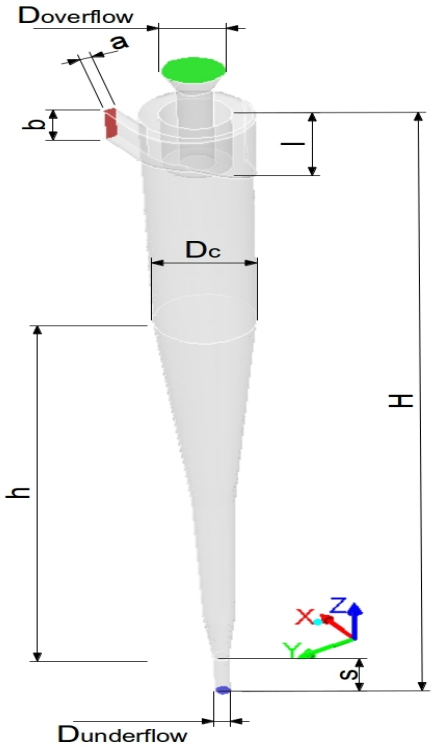

Figure 1: Cyclone Geometry.

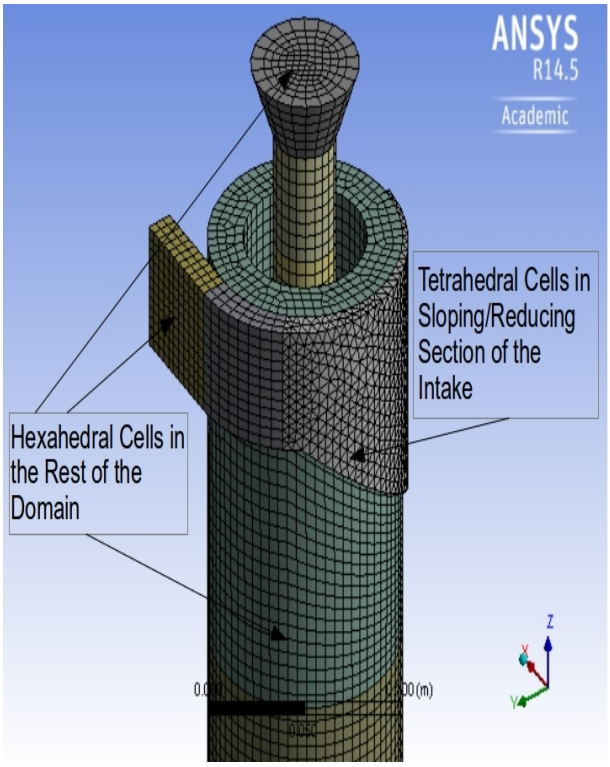

Figure 2: Computational Grid (Mesh).

Table 2: Hydrocyclone dimensions.

D_c (mm)	H (mm)	$D_{overflow}$ (mm)	$D_{underflow}$ (mm)	h (mm)	l (mm)	s (mm)	a (mm)	b (mm)
100	1250	75	20	895	80	100	13	45

LBM Model

LBM Model Geometry and Domain Voxelisation

The LBM models were implemented using the Palabos open-source libraries [15]. Palabos does not have a dedicated pre-processor for geometry creation and voxelisation (the LBM equivalent of meshing). Thus, a multitude of codes were used to generate the geometry and voxelise the computational domain. The first step was to export the geometry created in the ANSYS Fluent pre-processor (DesignModeller) as an initial graphics exchange specification (IGES) file. The IGES file was imported into Solidworks [16] and converted to a stereo-lithography (STL) file as seen in Figure 3.

The STL file contains a triangular mesh representation of the surface of the hydrocyclone including the inlet and outlets. Palabos requires that the STL file have holes instead of surfaces for the inlet and outlets. Thus, MeshLab [17] was used to create holes (open faces) in the place of the inlet and outlets. MeshLab was also used to clean any non-manifold faces or vertices in the STL file. A bounding box, as seen in Figure 3, was created around the STL file to specify the computational domain.

Table 3: Flow Boundary conditions.

Boundary Name	Boundary Type	Pressure (kPa)	$\dot{m}$ (kg/s)	D_H (m)	I_{turb} (%)
Inlet	Mass-flow inlet	$P_a + 62.5$	5.67	0.02	8.86
Underflow	Pressure outlet	P_a	N/A	0.02	10
Overflow	Pressure outlet	P_a	N/A	0.075	10

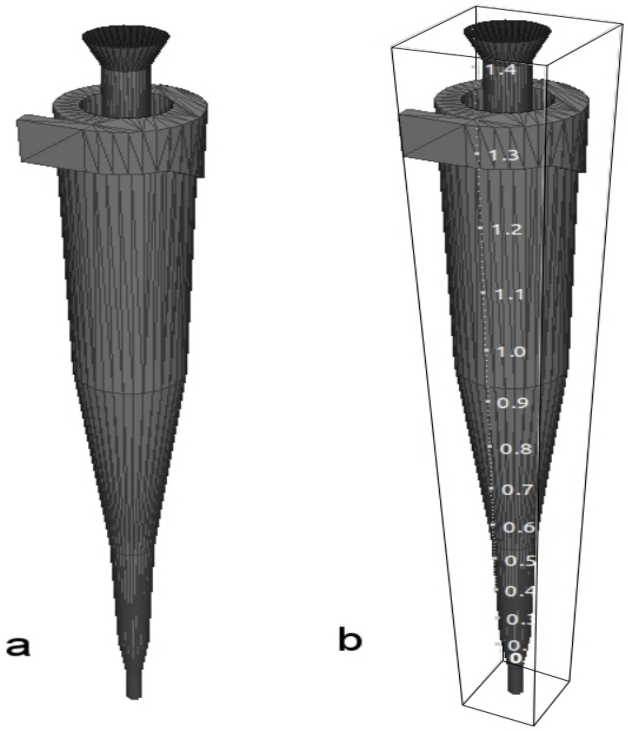

Figure 3: Wall surface and domain construction via STL - a) hydrocyclone and b) bounding box around the hydrocyclone.

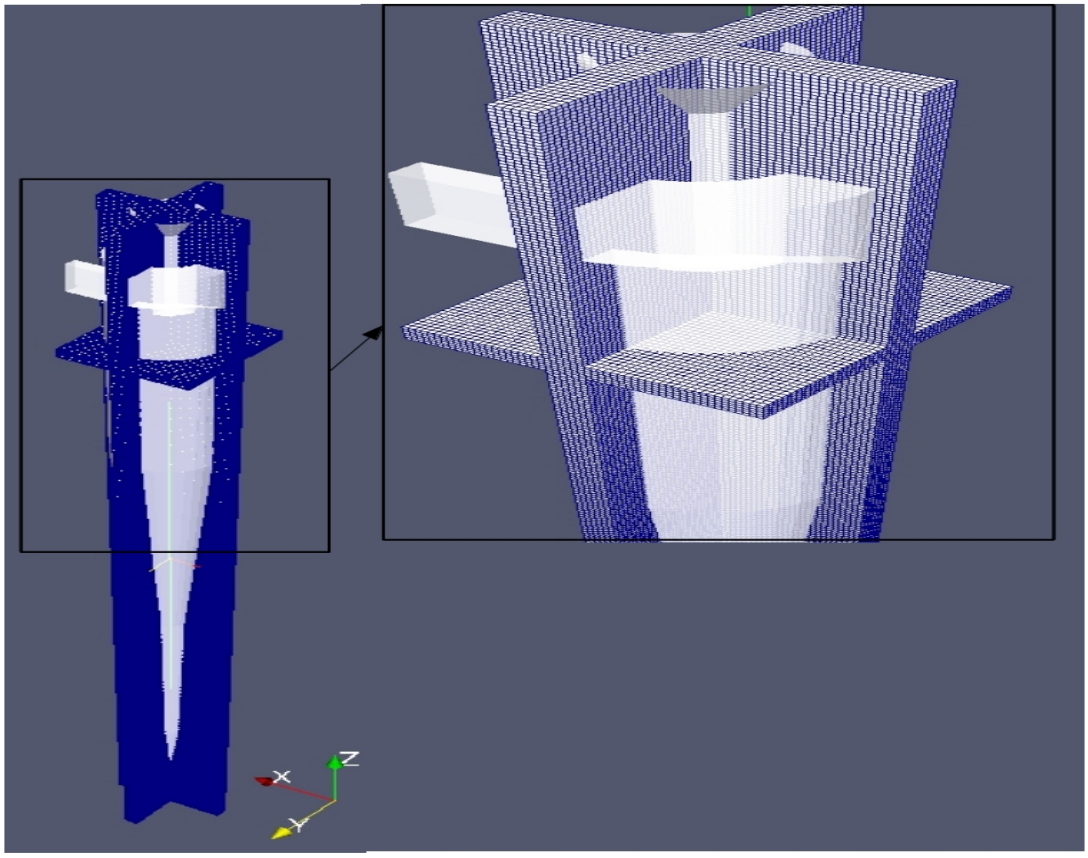

Figure 4: Section of the voxelised domain.

The domain is voxelised using Palabos. This is done as part of the simulation by specifying the x, y and z resolution (grid spacing) which creates a voxelised domain within the bounding box. The resolution in all three directions was 600. This produced a mesh of 1.82349 million lattices (cells). The cells that were outside of the cyclone made up 17% of the cells. The time step size was $\delta_t = 2.66(10^{-5})\ s$.

The sectioned voxelised domain is shown in Figure 4. Each cubic cell in Figure 4 is a lattice that is connected to each neighbouring lattice. Figure 4 was generated using Paraview [18]. The STL file is used by Palabos to define the domain, wall boundaries as well as the inlet and outlets.

LBM Governing Equations and Boundary Conditions

The single relaxation time (SRT) Bhatnagar-Gross-Krook (BGK) LBM model is used. This is commonly referred to as the BGK-LBM. Thus, the Boltzmann equation is given as [19]:

$$\frac{\partial f}{\partial t} + \xi.\nabla f + \mathbf{g}.\nabla_\xi f = -\frac{1}{\tau_*}(f - f^{eq}) \tag{4}$$

The equilibrium distribution function is given by the truncated Taylor expansion of the Maxwellian distribution function [20]:

$$f_{eq} = w_i \rho \left[1 + \frac{\mathbf{c}_i.\mathbf{u}}{c_s^2} + \frac{(\mathbf{c}_i.\mathbf{u})^2}{2c_s^4} - \frac{u^2}{2c_s^2}\right] \tag{5}$$

where $c_s = 1/\sqrt{3}c$. The $D3Q19$ lattice was used [20]. In the LBM the pressure is $p = c_s^2 \rho$ [20]. The relaxation time with a viscosity correction to include the Static Smagorinsky LES model is given by [21]:

$$\tau_* = \tau_o + \tau_t = \left(\frac{\nu}{c_s^2} + \frac{1}{2}\right) + \left(\frac{(C_s \Delta x)^2}{c_s^2 \delta_t}|S|\right) \tag{6}$$

where $C_s = 0.14$.

The cells, within the bounding box, that were outside of the hydrocyclone domain were assigned no-dynamics. Thus, the distribution functions for the no-dynamics cells were set to zero. The inlet was specified as a velocity inlet with the velocity specified to obtain the mass-flow rate given in Table 3. The inlet was specified as a pressure inlet matching that in Table 3. The outlets were specified as pressure outlets matching that in Table 3. The wall boundaries were assigned using the Guo off-lattice boundary scheme proposed by Guo, Chuguang and Baochang [22], which reproduced a no-slip boundary at the walls.

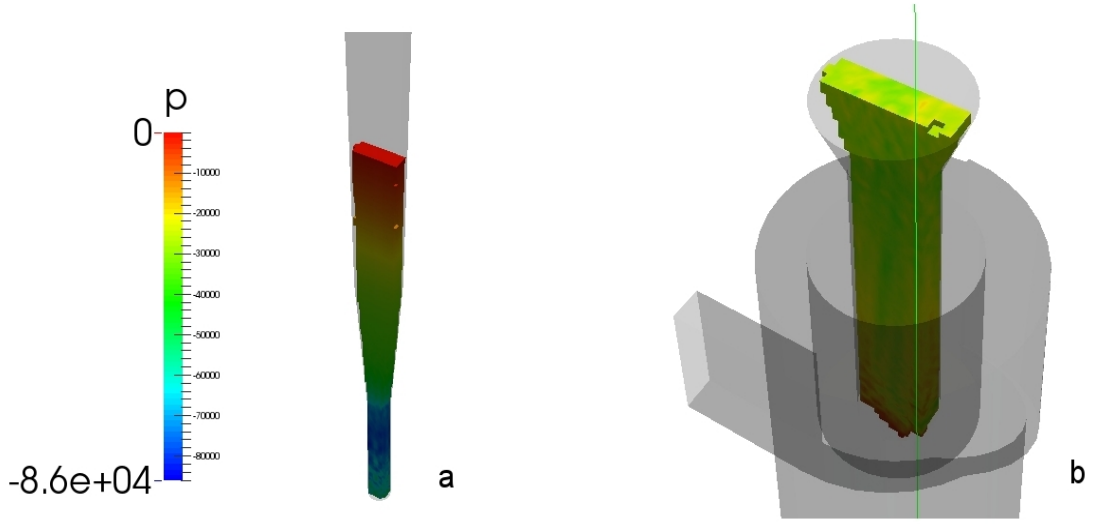

Figure 5: Contours coloured by pressure (Pa) - LBM predictions - at the a) underflow and b) overflow.

Results

The LBM model does predict a low (suction) pressure at the underflow and overflow as seen in Figure 5. The low pressure at the underflow and overflow is the primary mechanism for air-core formation in hydrocyclones. This indicates that the LBM can be used to predict air-core formation in hydrocyclones. However, the low pressure region predicted in the LBM does not run completely through the core of the hydrocyclone. Based on existing literature [23] the low pressure region does run through the entire core of the hydrocyclone.

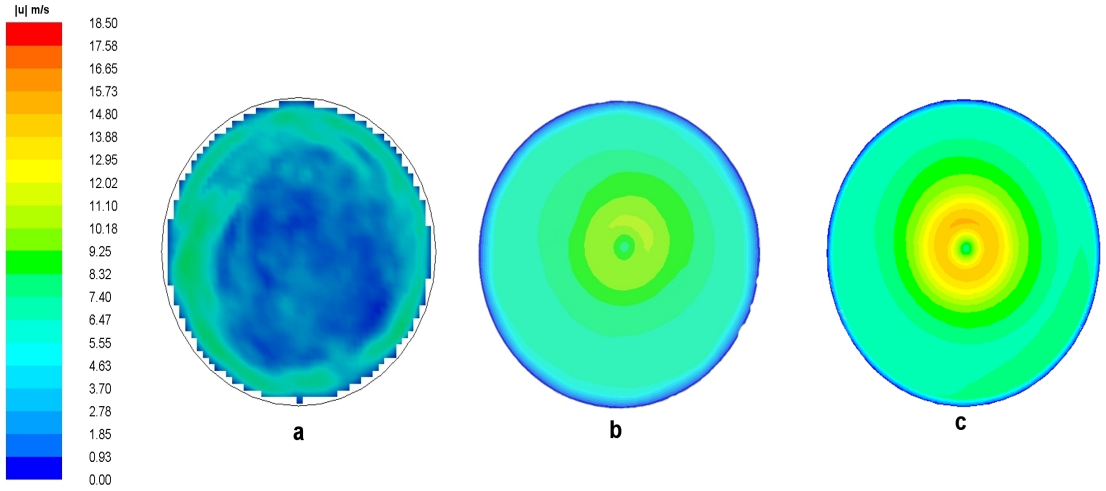

Figure 6: Contours coloured by velocity magnitude ($|\mathbf{u}|\ m/s$) on the planes $z = 0$ for the a) LBM model, b) NS model (124000 cells) and c) NS model (920000 cells).

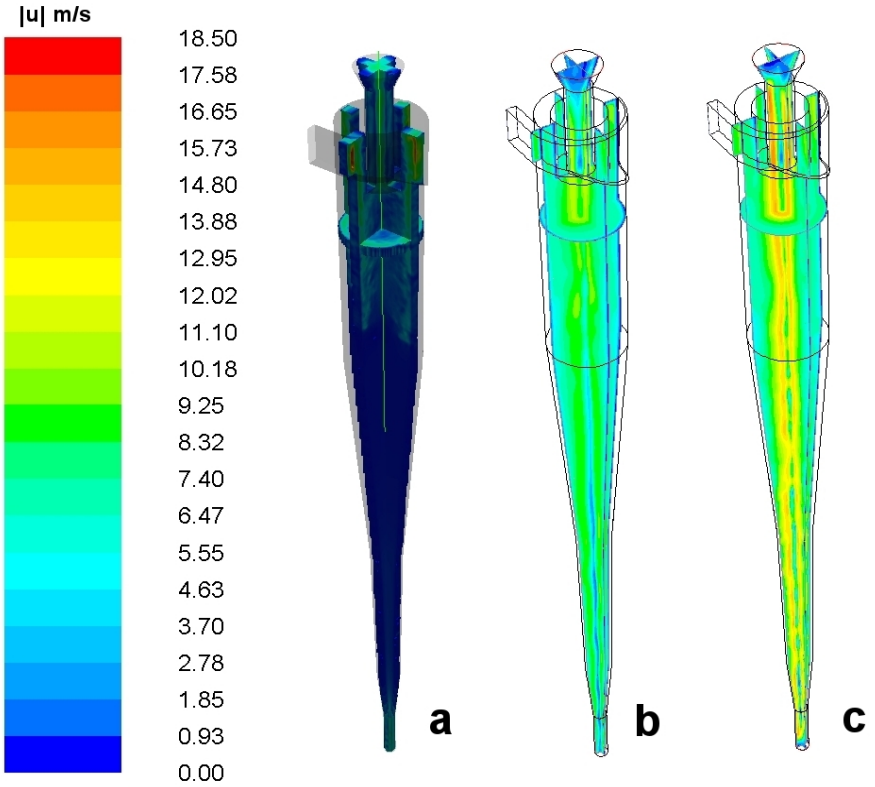

Figure 7: Contours coloured by velocity magnitude ($|\mathbf{u}|\ m/s$) on the planes $x = 0$, $y = 0$ and $z = 0$ for the a) LBM model, b) NS model (124000 cells) and c) NS model (920000 cells).

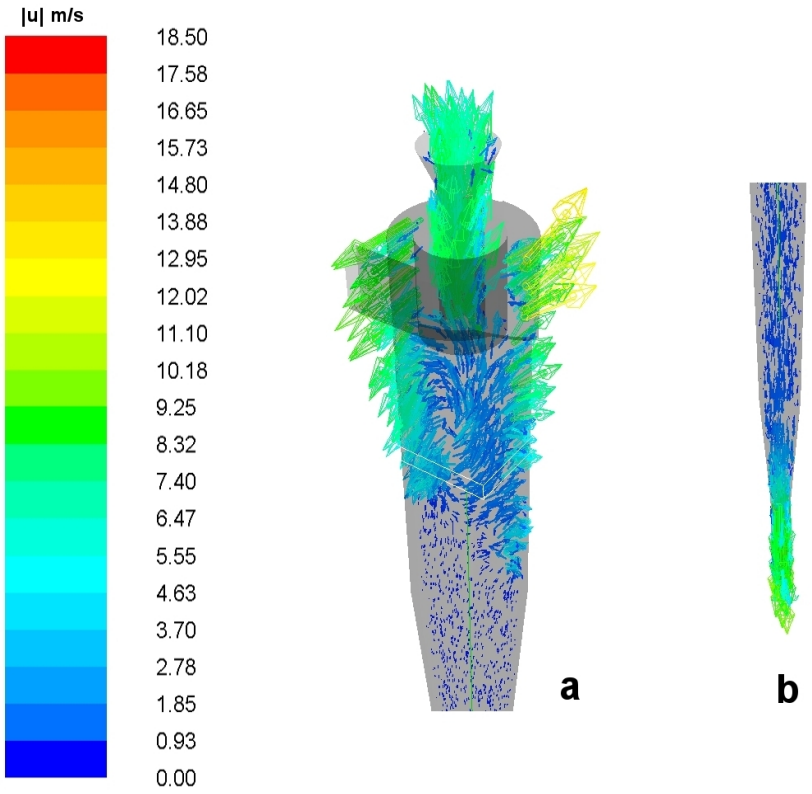

Figure 8: Vectors coloured by velocity magnitude ($|\mathbf{u}|$ m/s) in the a) upper section and b) lower section of the hydrocyclone for the LBM.

The missing low pressure region in the LBM model may relate to the fact that the LBM model does not predict a high velocity region in the core of the hydrocyclone. Figure 6 illustrates that away from the core of the hydrocyclone the LBM predictions are comparative to the NS model predictions. However, in the core of the hydrocyclone the LBM model do not predict the high velocity region as seen in the NS based model.

The LBM predicts higher velocities, than the NS model, in the cylindrical section of the hydrocyclone as seen in Figure 7. Figure 7 also shows that the LBM predicts significantly lower velocities than the NS model in the conical section of the hydrocyclone. As seen in Figures 6 and 7 the NS model with the finer mesh predicts higher velocities, in the core of the hydrocyclone, than the NS model with the coarse mesh. Despite the differences between the LBM and NS predictions in the conical section, the LBM predicts the correct rotational flow structure in the upper section and in the spigot as seen in Figure 8.

The LBM simulation employed between 2-15 times as many lattices as opposed to the number of cells in the NS models. This was necessary to obtain comparable results. However, the computational requirements for the LBM were not excessively high. Due to the high level of parallelism inherent in the LBM, the LBM models were executed on an Intel Core i7 based quad core laptop, using eight threads via hyper-threading and 6 GB RAM. The LBM simulations used an hour of computation time. In comparison the NS models were executed on a PC with an Intel Core i7 quad core (eight threads) and 24 GB RAM as well as the Centre for High Performance Computing (CHPC) Dell Westmere Intel Xeon based cluster (120 physical cores). The 124000 cell NS model ran for two weeks on the PC. The 920000 cell model ran on the PC initially but required fifty days computation time. Thus, it was placed on the cluster which took two days to run. This clearly illustrates the potential for the LBM to address the issue of large computational requirements for high resolution CFD solutions.

Conclusions and Recommendations

An LBM model of a hydrocyclone using the SRT approach is presented. The model incorporated the static Smagorinsky LES turbulence model. The LBM model is compared to predictions from an NS based FVM model. The model and its' implementation is outlined in detail.

The LBM model predicts velocities in the cylindrical section of the hydrocyclone and vortex finder that are in close agreement with the NS model. However, the LBM model predicts significantly lower velocities in

the cone section of the hydrocyclone and in the core of the hydrocyclone. The LBM predicts the low pressure region at the underflow and overflow. However, the LBM model does not display the low pressure region in the core of the hydrocyclone which is predicted by the NS model. This low pressure region is partly responsible for air-core formation.

A similar model as Pirker *et al.* [5] was used for the LBM simulation. This source showed that the LBM predicts lower velocities in the core of the cyclone. The LBM model in the source paper proved suitable for short cut flow. This is the same thing observed in the results in this study. Thus, it appears that this implementation of the LBM may be suitable for modelling short cut flow. However, certain modifications need to be made to the LBM used in the source and in our paper to account for non-short cut hydrocyclone flow.

The regions of concern are the high velocity regions. It is proposed that these differences are related to the use of the SRT implementation of the LBM, which may not be suitable for high-Reynolds number flows. The possible solution is to use the multiple relaxation time (MRT) model which is more suitable to high-Reynolds number flow. The MRT-LBM model of the hydrocyclone is currently being implemented.

Furthermore, Brennan, Holtham and Narasimha [23] found that in the case of a coarse mesh, as used in the CFD in this study, the RSM is more accurate than the LES. A coarse mesh is used in this work, thus, the RSM model is used. It would be more appropriate to use the LES for finer meshes which is reserved for future work.

Acknowledgements

The financial assistance (scholarships) of the National Research Foundation (NRF) and the University of Johannesburg Next Generation Scholarship (UJ NGS) towards this research is hereby acknowledged. The Centre for High Performance Computing (CHPC) is acknowledged for the use of the CHPC facilities. The support and encouragement of Multotec Pty Ltd in the pursuit of this research is also acknowledged. Opinions expressed and conclusions arrived at, are those of the authors and cannot necessarily be attributed to the NRF, the University of Johannesburg (UJ), the CHPC or Multotec Pty Ltd.

References

1. H. E. Van den Akker, “Toward a Truly Multiscale Computational Strategy for Simulating Turbulent Two-Phase Flow Processes,” *Industrial and Engineering Chemistry Research*, vol. 49, pp. 10 780–10 797, 2010.

2. L. Wang, B. Zhang, X. Wang, W. Ge, and J. Li, “Lattice Boltzmann Based Discrete Simulation for Gas-Solid Fluidization,” *Chemical Engineering Science*, vol. 101, pp. 228–239, 2013.

3. H. Gao, H. Li, and L. Wang, “Lattice Boltzmann Simulation of Turbulent Flow Laden with Finite-Size Particles,” *Computers and Mathematics with Applications*, vol. 65, pp. 194–210, 2013.

4. G. Gronald and J. Derksen, “Simulating Turbulent Swirling Flow in a Gas cyclone: A Comparison of Various Modeling Approaches,” *Powder Technology*, vol. 205, pp. 160–171, 2011.

5. S. Pirker, C. Goniva, C. Kloss, S. Puttinger, J. Houben, and S. Schneiderbauer, “Application of a Hybrid Lattice Boltzmann - Finite Volume Turbulence Model to Cyclone Short-Cut Flow,” *Powder Technology*, vol. 235, pp. 572–580, 2013. [Online]. Available: http://dx.doi.org/10.1016/j.powtec.2012.10.035

6. ANSYS, Inc., *ANSYS Fluent 14.5. [DVD-ROM].*, Canonsburg, PA : USA, October 2012.

7. S. Patankar, *Numerical Heat Transfer and Fluid Flow*, 1st ed. Minnesota: Hemisphere Publishing Corporation, 1980.

8. K. Versteeg and W. Malalasekera, *An Introduction to Computational Fluid Dynamics : The Finite Volume Method*, 1st ed. Essex: Longman Scientific and Technical, 1995.

9. R. Ansorge, *Mathematical Models of Fluid Dynamics: Modelling, Theory, Basic Numerical Facts âĂŞ An Introduction*, 1st ed. Hamburg: WILEY-VCH GmbH & Co. KGaA, Weinheim, Inc., 2003.

10. ANSYS Fluent Technical Staff, *ANSYS Fluent 14.5. Theory Guide, ANSYS Inc.*, ANSYS Inc., Canonsburg, PA : USA, October 2012.

11. D. Kuzmin, *Introduction to Computational Fluid Dynamics, Lecture 1 - Lecture 11*, University of Dortmund - Institute of Applied Mathematics. [Online]. Available: http://www.mathematik.uni-dortmund.de/~kuzmin/cfdintro/cfd.html

12. R. Blevins, *Applied Fluid Dynamics Handbook*, 1st ed. NY: Van Nostrand Reinhold Company, Inc., 1984.

13. D. Wilcox, *Turbulence Modelling for CFD*, 2nd ed. Glendale, CA: Griffin Printing, Inc., 1994.

14. ANSYS Fluent Technical Staff, *ANSYS Fluent 14.5. Users Guide, ANSYS Inc.*, ANSYS Inc., Canonsburg, PA : USA, October 2012.

15. Flowkit Ltd., *Palabos 1.4r1.*, Lausanne: Switzerland, May 2013. [Online]. Available: http://www.palabos.org

16. Dassault Systémes SolidWorks Corporation, *Solidworks 2012-2013. [DVD-ROM].*, Waltham, MA: USA.

17. Visual Computing Lab - Istituto di Scienza e Tecnologie dell'Informazione "A. Faedo", *MeshLab v1.3.2*, Pisa: Italy, August 2012. [Online]. Available: http://meshlab.sourceforge.net/

18. Kitware, Inc, *Paraview 4.0.1*, NY: USA. [Online]. Available: http://www.paraview.org

19. H. Ling, L. Q. W. Yong, and T. G. Hai, "Lattice Boltzmann Method and its Applications in Engineering Thermophysics," *Chinese Sci. Bull.*, vol. 54, pp. 4117–4134, 2009.

20. M. Hecht and J. Harting, "Implementation of On-Site Velocity Boundary Conditions for $D3Q19$ Lattice Boltzmann Simulations," *Journal of Statistical Mechanics: Theory and Experiment*, vol. 2010, no. 01, p. P01018, 2010. [Online]. Available: http://stacks.iop.org/1742-5468/2010/i=01/a=P01018

21. H. Yu, S. S. Girimaji, and L. Luo, "DNS and LES of Decaying Isotropic Turbulence with and without Frame Rotation using Lattice Boltzmann Method," *Journal of Computational Physics*, vol. 209, pp. 599–616, 2005.

22. Z. Guo, C. Zheng, and B. Shi, "An Extrapolation Method for Boundary Conditions in Lattice Boltzmann Method," *Phys. Fluids*, vol. 14, pp. 2007–2010, 2002.

23. M. Narasimha, M. Brennan, and P. Holtham, "Large Eddy Simulation of Hydrocyclone-Prediction of Air-Core Diameter and Shape," *International Journal of Mineral Processing*, vol. 80, pp. 1–14, 2006.